2012

Vortices in the extended Skyrme-Faddeev model

PHYSICAL REVIEW D, COLLEGE PK, v. 85, n. 10, supl. 2, Part 3, pp. 126-132, MAY 9, 2012
http://www.producao.usp.br/handle/BDPI/41874

PHYSICAL REVIEW D **85,** 105006 (2012)

Vortices in the extended Skyrme-Faddeev model

L. A. Ferreira,[1,*] J. Jäykkä,[2,†] Nobuyuki Sawado,[3,‡] and Kouichi Toda[4,§]

[1]*Instituto de Física de São Carlos; IFSC/USP; Universidade de São Paulo—USP, Caixa Postal 369, CEP 13560-970, São Carlos-SP, Brazil*

[2]*School of Mathematics, University of Leeds, LS2 9JT Leeds, United Kingdom*

[3]*Department of Physics, Tokyo University of Science, Noda, Chiba 278-8510, Japan*

[4]*Department of Mathematical Physics, Toyama Prefectural University, Kurokawa 5180, Imizu, Toyama, 939-0398, Japan*

(Received 1 March 2012; published 9 May 2012)

We construct analytical and numerical vortex solutions for an extended Skyrme-Faddeev model in a $(3 + 1)$ dimensional Minkowski space-time. The extension is obtained by adding to the Lagrangian a quartic term, which is the square of the kinetic term, and a potential which breaks the $SO(3)$ symmetry down to $SO(2)$. The construction makes use of an ansatz, invariant under the joint action of the internal $SO(2)$ and three commuting $U(1)$ subgroups of the Poincaré group, and which reduces the equations of motion to an ordinary differential equation for a profile function depending on the distance to the x^3 axis. The vortices have finite energy per unit length, and have waves propagating along them with the speed of light. The analytical vortices are obtained for a special choice of potentials, and the numerical ones are constructed using the successive over relaxation method for more general potentials. The spectrum of solutions is analyzed in detail, especially its dependence upon special combinations of coupling constants.

DOI: 10.1103/PhysRevD.85.105006 PACS numbers: 05.45.Yv, 81.07.De

I. INTRODUCTION

The so-called Skyrme-Faddeev model was introduced in the 1970s [1] as a generalization to $(3 + 1)$ dimensions of the $O(3)$ nonlinear sigma model in $(2 + 1)$ dimensions [2]. The Skyrme term, quartic in derivatives of the field, balances the quadratic kinetic term and, according to Derrick's theorem, allows the existence of stable solutions with nontrivial Hopf topological charges. Because of the highly nonlinear character of the model and the lack of symmetries, the first soliton solutions were only constructed in the late 1990s using numerical methods [3–6]. Since then, the interest in the model has increased considerably, and it has found applications in many areas of physics due mainly to the knotted character of the solutions [7]. The numerical efforts in the construction of the solutions have improved our understanding of the properties of the model [8], and even the scattering of knotted solitons has been investigated [9]. One of the aspects of the model that has attracted considerable attention has been its connection with gauge theories. Faddeev and Niemi have conjectured that it might describe the low energy limit of the pure $SU(2)$ Yang-Mills theory [10]. They based their argument on a decomposition of the physical degrees of freedom of the $SU(2)$ connection, proposed in the 1980s by Cho [11], and involving a triplet of scalar fields $\vec{n}$ taking values on the sphere S^2 ($\vec{n}^2 = 1$). The conjecture, which is quite controversial [12], states that the low energy effective action of the $SU(2)$ Yang-Mills theory is the Skyrme-Faddeev action, and the knotted solitons would describe glueballs or even vacuum configurations. The fact that the Skyrme-Faddeev model has an $O(3)$ symmetry, and so possesses Goldstone boson excitations, is one of the many difficulties facing the conjecture, and some modifications of it were in fact proposed [13]. Any check of such types of conjectures is of course very difficult to perform since it must involve nonperturbative calculations in the strong coupling regime of the Yang-Mills theory. However, Gies [14] has calculated the Wilsonian one loop effective action for the pure $SU(2)$ Yang-Mills theory assuming Cho's decomposition, and found that the Skyrme-Faddeev action is indeed part of it, but additional quartic terms in the derivatives of the triplet $\vec{n}$ are unavoidable. In fact, the first numerical Hopf solitons were first constructed for the Skyrme-Faddeev model modified by a quartic term [3] which is the square of the kinetic term. However, the soliton solutions in [3] were constructed for a sector of the theory where the signs of the coupling constants disagree with those indicated by Gies's calculations. The addition of quartic terms has the drawback of making the Lagrangian dependent on terms which are quartic in time derivatives, and so the energy is not positive definite. However, as a quantum field theory the Skyrme-Faddeev model is not renormalizable by power counting and has to be considered as a low energy effective theory. In addition, under the Wilsonian renormalization group flow the square of the kinetic term is as unavoidable as the Skyrme quartic term. Therefore, it is quite natural to investigate the properties of the Skyrme-Faddeev model with such modifications.

In this paper we consider an extended Skyrme-Faddeev model defined by the Lagrangian

*laf@ifsc.usp.br
†juhaj@iki.fi
‡sawado@ph.noda.tus.ac.jp
§kouichi@yukawa.kyoto-u.ac.jp

$$\mathcal{L} = M^2 \partial_\mu \vec{n} \cdot \partial^\mu \vec{n} - \frac{1}{e^2}(\partial_\mu \vec{n} \wedge \partial^\mu \vec{n})^2 - V(n_3), \quad (1.1)$$

where $\vec{n}$ is a triplet of real scalar fields taking values on the sphere S^2, M is a coupling constant with dimension of $(\text{length})^{-1}$, e^2 and β are dimensionless coupling constants, and the potential is a functional of the third component n_3 of the triplet $\vec{n}$. Note that the potential breaks the $O(3)$ symmetry of the original Skyrme-Faddeev model down to $O(2)$, the group of rotations on the plane $n_1 n_2$, thus eliminating two of the three Goldstone boson degrees of freedom. In this paper the main role of the potential is to stabilize the vortex solutions.

The first exact vortex solutions for the theory (1.1) were constructed in [15] for the case where the potential vanishes, and by exploring the integrability properties of a submodel of (1.1). In order to describe those exact vortex solutions it is better to perform the stereographic projection of the target space S^2 onto the plane parametrized by the complex scalar field u and related to $\vec{n}$ by

$$\vec{n} = (u + u^*, -i(u - u^*), |u|^2 - 1)/(1 + |u|^2). \quad (1.2)$$

It was shown in [15] that the field configurations of the form

$$u \equiv u(z, y), \qquad u^* \equiv u^*(z^*, y) \quad \text{for } \beta e^2 = 1, \qquad V = 0 \quad (1.3)$$

are exact solutions of (1.1), where $z = x^1 + i\varepsilon_1 x^2$ and $y = x^3 - \varepsilon_2 x^0$, with $\varepsilon_a = \pm 1$, $a = 1, 2$, and x^μ, $\mu = 0, 1, 2, 3$, are the Cartesian coordinates of the Minkowski space-time. Despite the fact that (1.3) constitutes a very large class of solutions, no finite energy solutions were found within it. If the dependence of the u field upon the variable y is in the form of phases like e^{iky}, then one finds solutions with finite energy per unit of length along the x^3 axis. The simplest solution is of the form $u = z^n e^{iky}$, with n an integer, and it corresponds to a vortex parallel to the x^3 axis and with waves traveling along it with the speed of light. More general solutions of the class (1.3) were constructed in [16], including multivortices separated from each other and all parallel to the x^3 axis. The ideas of [15] were generalized to an extended Skyrme-Faddeev model defined on the target space CP^N, possessing $N - 1$ complex scalar fields u_i, and the class of solutions constructed is like (1.3), where the fields u_i are arbitrary functions of z and y [17]. Note that the solutions (1.3) are not solutions of the original Skyrme-Faddeev model, since that corresponds to $\beta = 0$, and (1.3) requires the condition $\beta e^2 = 1$. If one takes the limit $\beta \to 0$ and $\frac{1}{e^2} \to 0$, keeping the product βe^2 constant and equal to unity, one observes that (1.1) reduces to the CP^1 model (if $V = 0$). Therefore, the configurations (1.3) are also solutions of the four dimensional CP^1 model. The ideas of [17] were then used to construct multi-vortex solutions for the four dimensional CP^N model [18,19]. Approximate vortex solutions for the pure Skyrme-Faddeev model, without the potential and β terms in (1.1), were constructed in [20].

The static energy density ($\mathcal{H}_{\text{static}} = -\mathcal{L}$) associated with (1.1) is positive definite if $V > 0$, $M^2 > 0$, $e^2 > 0$, and $\beta < 0$, that is, the sector explored in [3] and where Hopf soliton solutions were first constructed (for $V = 0$). In addition, this is also the sector explored in [21] but with additional terms involving second derivatives of the $\vec{n}$ field, and where Hopf solitons were also constructed. The static energy density of (1.1) is also positive definite for $V > 0$ if

$$M^2 > 0; \qquad e^2 < 0; \qquad \beta < 0; \qquad \beta e^2 \geq 1. \quad (1.4)$$

That is the sector that agrees with the signature of the terms in the one loop effective action calculated in [14] and that we will consider in this paper. Static Hopf solitons were constructed in [22,23] for the sector (1.4) (with $V = 0$), and their quantum excitations, including comparison with the glueball spectrum, were considered in [24]. An interesting feature of the Hopf solitons constructed in [22] is that they shrink in size and then disappear as $\beta e^2 \to 1$, which is exactly the point where the vortex solution of the class (1.3) exists.

The aim of the present paper is to investigate if vortex solutions for the model (1.1) continue to exist when the condition $\beta e^2 = 1$ is relaxed and, thus, if they coexist with the Hopf solitons in [22]. We also aim at the study of their properties and stability. The idea is to keep the solutions as close to those of the class (1.3) as possible. In order to do that, we follow the ideas of [25] and implement an ansatz based on the $O(2)$ internal symmetry given by the transformations $u \to e^{i\alpha} u$, together with three commuting transformations of the Poincaré group given by rotations on the plane $x^1 x^2$, and translations in the directions x^0 and x^3. We impose the field configurations to be invariant under the diagonal subgroups of the tensor product of the internal $O(2)$ group with each one of the three commuting one-parameter subgroups of the Poincaré group. The resulting ansatz is given by

$$u \equiv f(\rho) e^{i(n\varphi + \lambda z + k\tau)}, \quad (1.5)$$

where n is an integer for u to be single valued, and λ, k are real dimensionless parameters, and where we have used the dimensionless polar coordinates (ρ, φ, z, τ), defined by

$$\begin{aligned} x^0 &= ct = r_0 \tau, & x^1 &= r_0 \cos\varphi, \\ x^2 &= r_0 \sin\varphi, & x^3 &= r_0 z, \end{aligned} \quad (1.6)$$

and where we have introduced a length scale r_0 given by

$$r_0^2 = -\frac{4}{M^2 e^2} \quad (1.7)$$

which is positive since we are dealing with $e^2 < 0$ [see (1.4)]. Note that when $\lambda = \pm k$ and $f \sim \rho^{\pm n}$, the configurations (1.5) are of the type (1.3). The ansatz (1.5) is in fact a generalization to $(3 + 1)$ dimensions of the ansatz used in the baby Skyrme models [26,27].

The types of potentials we will consider in this part are of the form

$$V(n_3) \equiv \frac{\mu^2}{2}(1+n_3)^{2-(2/N)}(1-n_3)^{2+(2/N)}, \tag{1.8}$$

where N is a nonvanishing integer, and μ a real coupling constant. It is interesting to note that when the integer n of (1.5) has the same modulus as N of (1.8), one obtains analytical solutions of the form

$$u(\rho,\varphi,z,\tau) = \left(\frac{\rho}{a}\right)^N e^{i[N\varphi+k(z+\tau)]} \tag{1.9}$$

with $\varepsilon = \pm 1$, and where $a = |N|[\frac{(-e^2)(\beta e^2-1)M^4}{4\mu^2}]^{1/4}$. Such exact solutions are valid for all values of the coupling constants. In particular, for the case $\beta = 0$, (1.9) are exact solutions of the theory

$$\mathcal{L} = M^2\partial_\mu\vec{n}\cdot\partial^\mu\vec{n} - \frac{1}{e^2}(\partial_\mu\vec{n}\wedge\partial_\nu\vec{n})^2 - \frac{\mu^2}{2}(1+n_3)^{2-(2/N)}(1-n_3)^{2+(2/N)} \tag{1.10}$$

which is the proper Skyrme-Faddeev model in the presence of a potential. In this case we have $a = |N|[\frac{e^2M^4}{4\mu^2}]^{1/4}$ and $\mu^2e^2 > 0$.

In some cases we have been unable to find a numerical solution, which is expected in the analytical set, i.e. (1.9). Reasons for this are presented below. Apart from those cases, we have checked numerically the existence of the above solution. The numerical simulations are performed using a standard technique for a differential equation, the successive over relaxation (SOR) method. In order to further confirm the accuracy and correctness of the SOR code, some of the results were reproduced by an independent code using Newton's method, giving typical differences of the order of less than 10^{-4}.

The paper is organized as follows. In the next section we briefly describe the extended Skyrme-Faddeev model. The equations of motion are also introduced in Sec. II. We discuss the Hamiltonian density of the model in Sec. III. The method and the solutions of the integrable sector of the present model are discussed in Sec. IV. In Sec. V, we show the numerical solutions. Section VI is devoted to noting briefly potential physical applications of our solutions. A brief summary is presented in Sec. VII.

II. THE MODEL

In terms of the complex scalar field u introduced in (1.2), the Lagrangian (1.1) becomes

$$\mathcal{L} = 4M^2\frac{\partial_\mu u\partial^\mu u^*}{(1+|u|^2)^2} + \frac{8}{e^2}\left[\frac{(\partial_\mu u)^2(\partial_\nu u^*)^2}{(1+|u|^2)^4} + (\beta e^2-1)\frac{(\partial_\mu u\partial^\mu u^*)^2}{(1+|u|^2)^4}\right] - V(|u|^2), \tag{2.1}$$

where we have used the fact that n_3 is a functional of $|u|^2$ only, and so is the potential. The Euler-Lagrange equations following from (1.2), or (1.1), read

$$(1+|u|^2)\partial^\mu\mathcal{K}_\mu - 2u^*\mathcal{K}_\mu\partial^\mu u = -\frac{u}{4}(1+|u|^2)^3V', \tag{2.2}$$

where $V' = \frac{\partial V}{\partial|u|^2}$, and

$$\mathcal{K}_\mu \equiv M^2\partial_\mu u + \frac{4}{e^2}\frac{[(\partial_\nu u\partial^\nu u)\partial_\mu u^* + (\beta e^2-1)(\partial_\nu u\partial^\nu u^*)\partial_\mu u]}{(1+|u|^2)^2}. \tag{2.3}$$

We point out that the theory (2.1) possesses an integrable sector defined by the condition

$$(\partial_\mu u)^2 = 0. \tag{2.4}$$

Such a condition was first discovered in the context of the CP^1 model using the generalized zero curvature condition for integrable theories in any dimension [28], and then applied to many models with target space being the sphere S^2, or CP^1 (see [29] for a review). This leads to an infinite number of local conserved currents. Indeed, (2.4), together with the equations of motion (2.2), implies the conservation of the infinity of currents given by

$$J^G_\mu \equiv \mathcal{K}_\mu\frac{\delta G}{\delta u} - \mathcal{K}^*_\mu\frac{\delta G}{\delta u^*}, \tag{2.5}$$

where G is any functional of $|u|^2$ only. For the case where the potential vanishes, the set of conserved currents is considerably enlarged since G can be an arbitrary functional of u and u^*, but not of their derivatives. If, in addition to the condition (2.4), one takes $V = 0$ and $\beta e^2 = 1$, then the equations of motion reduce to $\partial^2 u = 0$. It is in that integrable sector that the solutions (1.3) lie, and they were studied in [15]. For theories defined by Lagrangians which are functionals of the Skyrme term only (pullback of the area form of the sphere) the currents of the form (2.5) are Noether currents associated with the area preserving diffeomorphisms of S^2 [30]. It is possible to define conditions weaker than (2.4) that lead to integrable theories associated with Abelian subgroups of the group of the area preserving diffeomorphisms [31].

Substituting the ansatz (1.5) into the equations of motion (2.2), we get an ordinary differential equation for the profile function f as

$$\frac{1}{\rho}\partial_\rho\left[\rho\frac{f'}{f}R\right] - \frac{(1-f^2)}{(1+f^2)}S\left[\Lambda - \left(\frac{f'}{f}\right)^2\right] = \frac{r_0^2}{4M^2}(1+f^2)^2\frac{\partial V}{\partial|u|^2}, \tag{2.6}$$

where the primes denote derivatives with respect to ρ, and where

$$\Lambda = \lambda^2 - k^2 + \frac{n^2}{\rho^2},$$
$$S = 1 + \beta e^2 \frac{f^2}{(1+f^2)^2}\left[\Lambda + \left(\frac{f'}{f}\right)^2\right], \tag{2.7}$$
$$R = 1 + \frac{f^2}{(1+f^2)^2}\left[(\beta e^2 - 2)\Lambda + \beta e^2\left(\frac{f'}{f}\right)^2\right].$$

With the choice of potential given in (1.8), we get that

$$\frac{r_0^2}{4M^2}(1+f^2)^2\frac{\partial V}{\partial \mid u \mid^2} = 2\frac{r_0^2\mu^2}{M^2}\left[\frac{(2-\frac{2}{N})(f^2)^{(1-2/N)} - (2+\frac{2}{N})(f^2)^{(2-2/N)}}{(1+f^2)^3}\right]. \tag{2.8}$$

We look for solutions satisfying the following boundary conditions:

$$\vec{n} \to \begin{cases} (0,0,-1) & \text{for } \rho \to 0 \\ (0,0,+1) & \text{for } \rho \to \infty, \end{cases} \tag{2.9}$$

which imply that the profile function should satisfy

$$f \to 0 \quad \text{for } \rho \to 0 \quad \text{and} \quad f \to \infty \quad \text{for } \rho \to \infty. \tag{2.10}$$

Let us then assume the following behavior of the profile function:

$$f = \begin{cases} \alpha_0 \rho^{s_1}(1 + \alpha_1\rho + \alpha_2\rho^2 \ldots) & \text{for } \rho \to 0 \\ \beta_0 \rho^{s_2}(1 + \beta_1 \frac{1}{\rho} + \beta_2 \frac{1}{\rho^2} \ldots) & \text{for } \rho \to \infty, \end{cases} \tag{2.11}$$

where $s_i > 0$, $i = 1, 2$. Substituting that into Eq. (2.6), one gets that the behavior for small ρ implies

$$s_1^2 = n^2, \tag{2.12}$$

where n is the integer in the ansatz (1.5). The behavior of (2.6) for large ρ implies that the relation between n^2 and s_2^2 depends upon the form of the potential, and

$$\lambda^2 - k^2 = \begin{cases} 8\frac{r_0^2\mu^2}{M^2} & \text{for } N = -1 \\ -2\frac{r_0^2\mu^2}{M^2} & \text{for } N = -2 \\ 0 & \text{for all other } N, \end{cases} \tag{2.13}$$

where N is the integer appearing in the potential (1.8), and λ, k are the parameters of the ansatz (1.5). Therefore, except for the cases $N = -1$ and $N = -2$, the waves along the vortex have to travel with the speed of light since the dependency upon x^3 and x^0 has to be of the form $x^3 \pm ct$. For the dimensionfull constants $L :== r_0\lambda$ and $K :== r_0 k$, the velocity is defined as

$$\frac{Kc}{L} = \begin{cases} \frac{Kc}{\sqrt{K^2+8\mu^2/M^2}} < c & \text{for } N = -1 \\ \frac{Kc}{\sqrt{K^2-2\mu^2/M^2}} > c & \text{for } N = -2. \end{cases} \tag{2.14}$$

Therefore, the mode is tachyonic for $N = -2$. $N = -1$ is not tachyonic, but the energy diverges from the boundary behavior of the potential. In the following analysis, we will concentrate on the analysis for $N \geqq 1$ (thus $\lambda^2 = k^2$).

III. THE ENERGY

The Hamiltonian density associated with (2.1) is not positive definite due to the quartic terms in time derivatives. We shall arrange the Legendre transform of each term in (2.1) to make explicit such nonpositive contributions, and write the Hamiltonian density as (see [32] for details)

$$\begin{aligned}\mathcal{H} = {} & 4M^2\frac{[\mid \dot{u} \mid^2 + \vec{\nabla}u\cdot\vec{\nabla}u^*]}{(1+\mid u\mid^2)^2} \\ & - \frac{24}{e^2}\frac{(\vec{\nabla}u)^2(\vec{\nabla}u^*)^2}{(1+\mid u\mid^2)^4}\left[\left(\frac{2}{3}\right)^2 - F^2\right] \\ & - 24\frac{(\beta e^2 - 1)}{e^2}\frac{[\mid \dot{u} \mid^2 + \frac{1}{3}\vec{\nabla}u\cdot\vec{\nabla}u^*][\vec{\nabla}u\cdot\vec{\nabla}u^* - \mid \dot{u}\mid^2]}{(1+\mid u\mid^2)^4} \\ & + V(\mid u\mid^2),\end{aligned} \tag{3.1}$$

where $\dot{u}$ denotes the x^0 derivative of u, and $\vec{\nabla}u$ its spatial gradient, and where we have denoted

$$\frac{\dot{u}^2}{(\vec{\nabla}u)^2} \equiv \frac{1}{3} + Fe^{i\Phi} \tag{3.2}$$

with $F > 0$ and $0 \leq \Phi \leq 2\pi$ being functions of the spacetime coordinates. Note that $\mathcal{H}$ given in (3.1) is positive definite for static configurations and for the range of parameters given in (1.4).

Using the ansatz (1.5) and the coordinates (1.6), we get $\dot{u} = iku/r_0$. The metric on the spatial submanifold is given by $ds^2 = r_0^2(d\rho^2 + \rho^2 d\varphi^2 + dz^2)$, and so

$$(\vec{\nabla}u)^2 = \frac{u^2}{r_0^2}(\Omega_- - \lambda^2), \qquad \vec{\nabla}u\cdot\vec{\nabla}u^* = \frac{f^2}{r_0^2}(\Omega_+ + \lambda^2), \tag{3.3}$$

where

$$\Omega_\pm = \left(\frac{f'}{f}\right)^2 \pm \frac{n^2}{\rho^2}. \tag{3.4}$$

In addition one gets that $\frac{\dot{u}^2}{(\vec{\nabla}u)^2} = \frac{1}{3} + Fe^{i\Phi} = -\frac{k^2}{(\Omega_- - \lambda^2)}$, and since it is real it follows that $\Phi = 0$ or π. Therefore, $(\frac{2}{3})^2 - F^2 = (\Omega_- - \lambda^2 - 3k^2)(\Omega_- + k^2 - \lambda^2)/3(\Omega_- - \lambda^2)^2$. So, the Hamiltonian density (3.1) becomes

$$\mathcal{H} = \frac{4}{r_0^4}\Big[M^2 r_0^2 \frac{f^2}{(1+f^2)^2}(\Omega_+ + \lambda^2 + k^2) + 2\frac{f^4}{(1+f^2)^4} \times \Big\{-\frac{1}{e^2}(\Omega_- - \lambda^2 - 3k^2)(\Omega_- + k^2 - \lambda^2) - \frac{(\beta e^2 - 1)}{e^2}(\Omega_+ + \lambda^2 + 3k^2)(\Omega_+ + \lambda^2 - k^2) + \mu^2 r_0^4 (f^2)^{-(2/N)}\Big\}\Big]. \tag{3.5}$$

IV. THE INTEGRABLE SECTOR

It is interesting to note that (2.6), (2.7), (2.8), and (2.9), with a special choice of the potential (1.8), have an analytical solution for each topological charge n. In fact, solutions of the integrable equation (2.4) also become the solutions of the present model. For $\lambda^2 = k^2$, the solutions can be written in the form

$$u(\rho, \varphi, z, \tau) = \left(\frac{\rho}{a}\right)^n e^{i[\varepsilon n\varphi + k(z+\tau)]}, \tag{4.1}$$

where $\varepsilon = \pm 1$, and a is a dimensionless constant to be fixed by the equations of motion. Substituting this into Eqs. (2.6), (2.7), (2.8), and (2.9), we get

$$\begin{aligned}(\beta e^2 - 1)\frac{4n^3}{a^4}&\left\{1 + \left(\frac{\rho}{a}\right)^{2n}\right\}^{-3}\left[(n-1)\left(\frac{\rho}{a}\right)^{2n-4} - (n+1)\left(\frac{\rho}{a}\right)^{4n-4}\right] \\ &= \frac{2r_0^2\mu^2}{M^2}\left\{1 + \left(\frac{\rho}{a}\right)^{2N}\right\}^{-3}\left[\left(2 - \frac{2}{N}\right)\left(\frac{\rho}{a}\right)^{2N-4} - \left(2 + \frac{2}{N}\right)\left(\frac{\rho}{a}\right)^{4N-4}\right].\end{aligned} \tag{4.2}$$

The constant a determines the scale of the vortex, and the equation is satisfied if $n = N$ and

$$a = |\,n\,|\left[\frac{M^2(\beta e^2 - 1)}{r_0^2\mu^2}\right]^{1/4} = |\,n\,|\left[\frac{(-e^2)(\beta e^2 - 1)M^4}{4\mu^2}\right]^{1/4}. \tag{4.3}$$

Thus, for all possible values of βe^2, we have analytical solutions. All those solutions satisfy the condition (2.4). Clearly, the class of solutions contains the special solution at $\beta e^2 = 1$ found previously in [15] if we take a proper limit of the vanishing potential, i.e. $\beta e^2 \to 1$ and $\mu^2 \to 0$, with $\frac{\beta e^2 - 1}{\mu^2} =$ constant. Also, apparently we have no solution at $\beta e^2 \neq 1$ without any potential because the scale (4.3) goes to infinity. Note that the case $\beta = 0$ is particularly interesting since it corresponds to the proper Skyrme-Faddeev model (without the extra quartic term) in the presence of a potential. Therefore, the configurations (4.1) are exact solutions of the theory (1.10) (for $n = N$), with $a = |\,N\,|\,[\frac{e^2M^4}{4\mu^2}]^{1/4}$ and $\mu^2 e^2 > 0$.

As we mentioned in Sec. II, for the sector satisfying (2.4), the model possesses the infinite set of conserved currents (2.5). In particular, choosing a form of $G = -4i(1 + |u|^2)^{-1}$, one gets the Noether current, associated to the phase transition by an arbitrary angle α, i.e., $u \to e^{i\alpha}u$,

$$J_\mu = -4iM^2\frac{u\partial_\mu u^* - u^*\partial_\mu u}{(1+|u|^2)^2} - i\frac{8}{e^2}(\beta e^2 - 1) \times \frac{2(\partial_\nu u\partial^\nu u^*)(\partial_\mu u^* u - u^*\partial_\mu u)}{(1+|u|^2)^4}. \tag{4.4}$$

For the solution (4.1), we can evaluate the charge per unit length for the solution

$$Q = \int dx_1 dx_2 J_0 = -8\pi M^2 k a^2 r_0\left[I(n) + \frac{n}{6}\frac{1}{a^2}(\beta e^2 - 1)\right], \tag{4.5}$$

where $I(n) = \frac{1}{n}\Gamma(1 + \frac{1}{n})\Gamma(1 - \frac{1}{n})$, with Γ being the Euler's Gamma function. Here we used an integral formula [33],

$$\int_0^\infty \frac{x^{\mu-1}dx}{(p + qx^\nu)^{m+1}} = \frac{1}{\nu p^{m+1}}\left(\frac{p}{q}\right)^{\mu/\nu}\frac{\Gamma(\frac{\mu}{\nu})\Gamma(1 + m - \frac{\mu}{\nu})}{\Gamma(1+m)}. \tag{4.6}$$

For the Hamiltonian (3.5), we perform similar computations. As a result, we get the energy per unit length by the integration on the x_1x_2 plane. For $n = 1$, the energy of the static vortex is (in units of $4M^2$)

$$E_{\text{static}} = 2\pi + \frac{4\pi}{3}\frac{1}{a^2}(\beta e^2 - 1), \tag{4.7}$$

and for $n \geq 2$ they are

$$E_{\text{static}} = 2\pi n + \frac{2\pi}{3}\frac{1}{a^2}(\beta e^2 - 1)(n^2 - 1)I(n). \tag{4.8}$$

Note that the first term is proportional to the topological charge. The energy per unit of length of the time-dependent vortex diverges for $n = 1$, and for $n \geqq 2$ we obtain

$$E_{\text{wave}} = 2\pi n + \frac{2\pi}{3}\frac{1}{a^2}(\beta e^2 - 1)(n^2 - 1)I(n) + k^2\left[2\pi a^2 I(n) + \frac{2\pi}{3}(\beta e^2 - 1)n\right]. \tag{4.9}$$

For the limit of $\beta e^2 \to 1$, $\mu^2 \to 0$, keeping $a^2 = n^2\sqrt{M^2(\beta e^2 - 1)/r_0^2\mu^2}$ finite, we obtain the energy per unit of length found previously in [15]. The energy monotonically grows as k^2 increases. Interestingly, the static vortex has a minimum at $\beta e^2 = 1.0$ and/or $\mu^2 = 0.0$, but for the time-dependent vortex there is a minimum of the energy for fixed βe^2 and k^2 and finite μ^2. The solutions are confirmed numerically in the subsequent section.

V. THE NUMERICAL ANALYSIS

Although the ansatz (1.5) is given in terms of the polar coordinates, for the numerical analysis it is more convenient to use a new radial coordinate y, defined by $\rho = \sqrt{\frac{1-y}{y}}$. Accordingly, we adopt a function g called the profile function, instead of using f, i.e., $f(\rho) = \sqrt{\frac{1-g(y)}{g(y)}}$.

Equation (2.6) can be promptly rewritten as

$$\frac{d}{dy}\left[\frac{y(1-y)}{g(1-g)}g'R\right]+\left(g-\frac{1}{2}\right)\frac{S}{y(1-y)}\left\{\Omega-\left(\frac{y(1-y)}{g(1-g)}g'\right)^2\right\} = -\frac{1}{y^2}\frac{r_0^2\mu^2}{M^2}(1-g)^{1-(2/N)}g^{1+(2/N)}\left\{4g-2\left(1+\frac{1}{N}\right)\right\}, \tag{5.1}$$

where the primes at this time indicate derivatives with respect to y and where

$$\Omega = (\lambda^2 - k^2)\frac{1-y}{y} + n^2, \tag{5.2}$$

$$S = 1 + \beta e^2 g(1-g)\frac{y}{1-y}\left\{\Omega + \left(\frac{y(1-y)}{g(1-g)}g'\right)^2\right\}, \tag{5.3}$$

$$R = 1 + g(1-g)\frac{y}{1-y}\left\{(\beta e^2 - 2)\Omega + \beta e^2\left(\frac{y(1-y)}{g(1-g)}g'\right)^2\right\}. \tag{5.4}$$

The energy in units of $4M^2$ per unit length for the time-dependent vortex can be estimated in terms of the following four parts of integrals of the dimensionless Hamiltonian $H :== \mathcal{H}/4M^2$,

$$E = 2\pi\int_0^\infty \rho d\rho H(\rho) = E_2 + E_4^{(1)} + (\beta e^2 - 1)E_4^{(2)} + \frac{r_0^2\mu^2}{M^2}E_0, \tag{5.5}$$

in which the components are defined as

$$E_2 = \pi\int_0^1 \frac{dy}{y(1-y)}\left\{(k^2+\lambda^2)\frac{1-y}{y} + n^2 + \left(\frac{y(1-y)}{g(1-g)}g'\right)^2\right\}g(1-g), \tag{5.6}$$

$$E_4^{(1)} = \pi\int_0^1 \frac{dy}{2(1-y)^2}\left\{(3k^2+\lambda^2)\frac{1-y}{y} + n^2 - \left(\frac{y(1-y)}{g(1-g)}g'\right)^2\right\}\left\{(k^2-\lambda^2)\frac{1-y}{y} + n^2 - \left(\frac{y(1-y)}{g(1-g)}g'\right)^2\right\}(g(1-g))^2, \tag{5.7}$$

$$E_4^{(2)} = \pi\int_0^1 \frac{dy}{2(1-y)^2}\left\{(3k^2+\lambda^2)\frac{1-y}{y} + n^2 + \left(\frac{y(1-y)}{g(1-g)}g'\right)^2\right\}\left\{(k^2-\lambda^2)\frac{1-y}{y} + n^2 + \left(\frac{y(1-y)}{g(1-g)}g'\right)^2\right\}(g(1-g))^2, \tag{5.8}$$

$$E_0 = 2\pi\int_0^1 \frac{dy}{y^2}g^{2+(2/N)}(1-g)^{2-(2/N)}. \tag{5.9}$$

For the integrable sector, we should choose $N = n$.

Generally speaking, a vortex is an object in three spatial dimensions; thus we have explored solutions in three spatial dimensions of (1.1). In the three spatial dimensions, the fourth order terms in the Lagrangian (including the

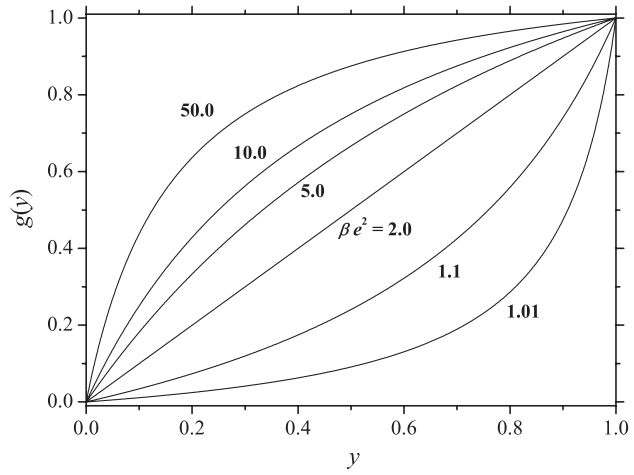

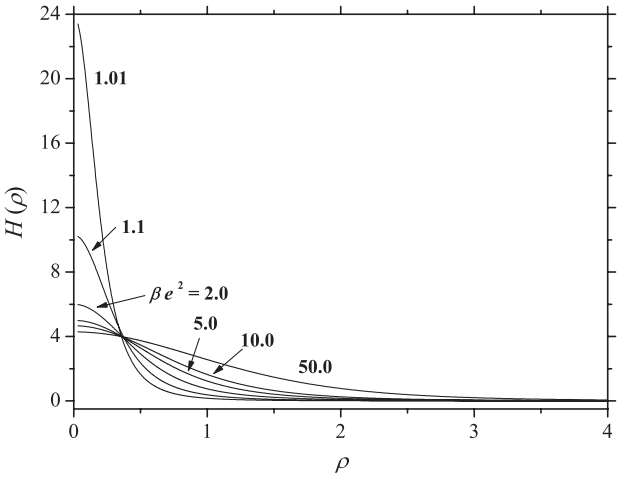

FIG. 1. The $n = 1$ profile $g(y)$ and the corresponding Hamiltonian density of the real space $H(\rho)$ of $k^2 = 0.0$ for the constant $r_0^2\mu^2/M^2 = 1.0$.

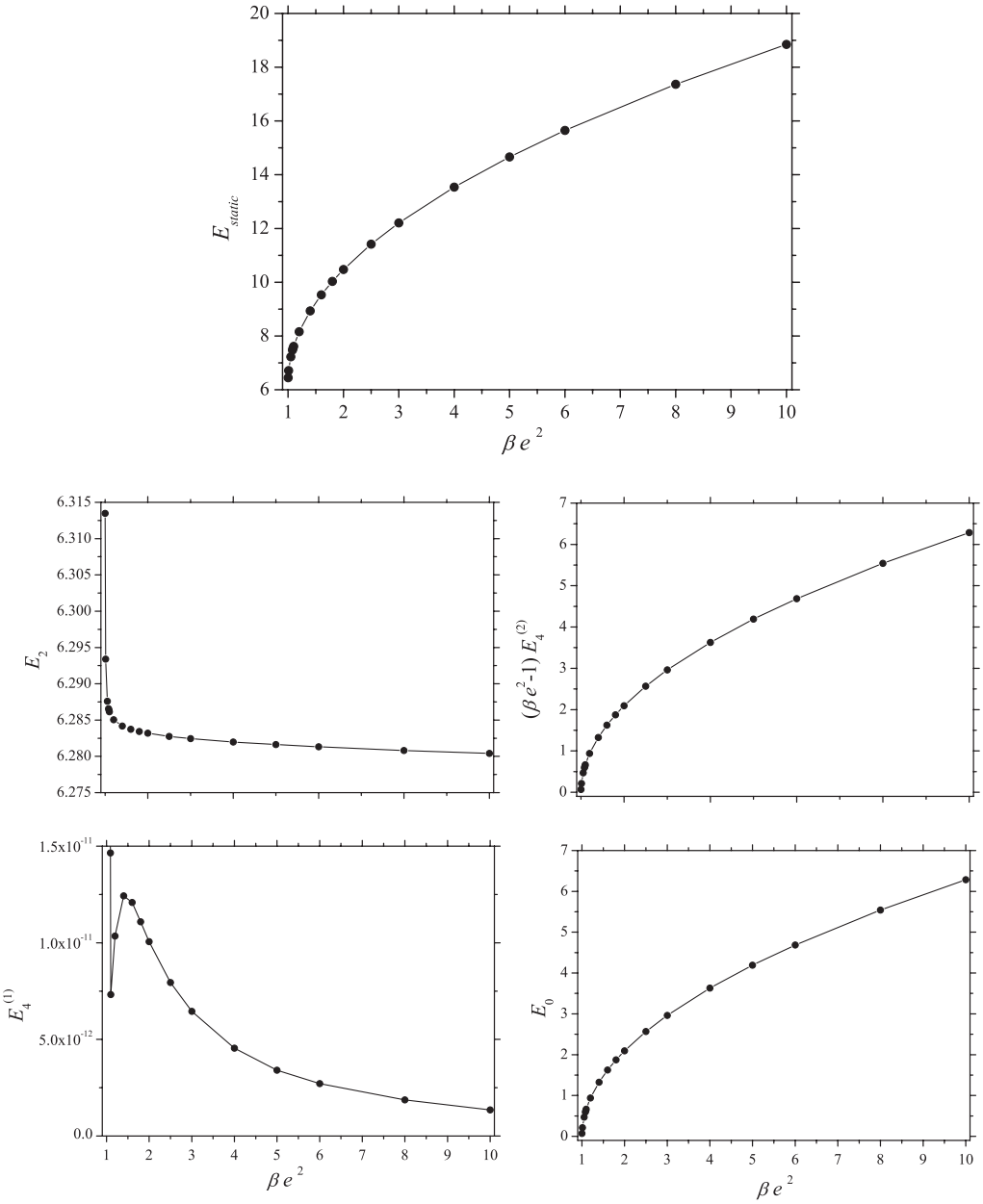

FIG. 2. The static energy and its components corresponding to the solutions of Fig. 1.

Skyrme term) successfully avoid the nonexistence theorem of static and finite energy solutions by Derrick. However, Eq. (2.6) of the ansatz (1.5) is the same as an equation of the corresponding static two spatial dimensions. This means the z component has no essential contribution to the stability. In fact, Derrick's theorem for two spatial dimensions implies that the contribution to the energy per unit length from quartic terms and the potential must be equal, namely,

$$E_4^{(1)} + (\beta e^2 - 1)E_4^{(2)} = \frac{r_0^2\mu^2}{M^2}E_0. \tag{5.10}$$

Since the solutions of the integrable sector satisfy $E_4^{(1)} = 0$, putting this together with $\beta e^2 = 1$ and $\mu^2 = 0$, one can confirm that the solution without the potential found in [15] satisfies the above condition automatically. This fact indicates that Derrick's argument to the energy per unit length also works well outside of the integrable sector.

The definition of the scale parameter a given in (4.3) indicates the existence of the analytical solution for the same sign of $\beta e^2 - 1$ and μ^2. In our previous study of Hopfions on the extended Skyrme-Faddeev model, we confirmed numerically that the solutions exist only for

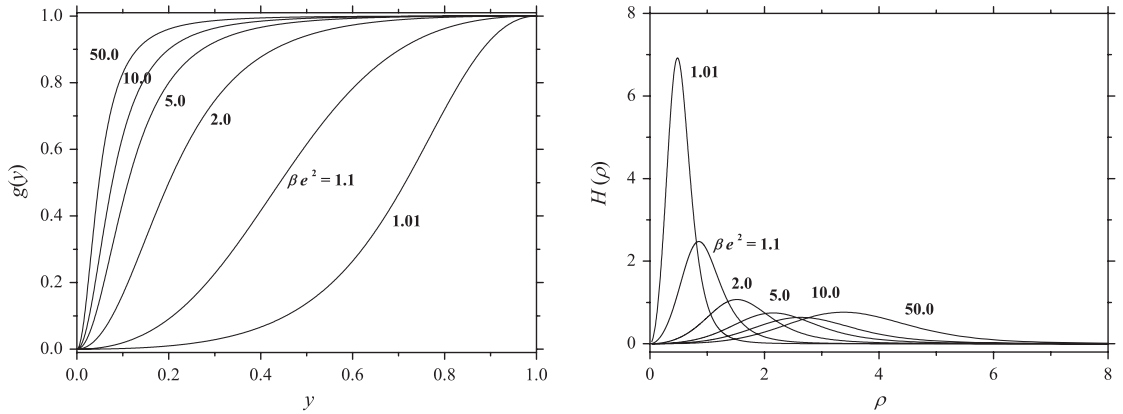

FIG. 3. The $n = 2$ profile $g(y)$ and the corresponding Hamiltonian density of the real space $H(\rho)$ of $k^2 = 0.0$ for the constant $r_0^2\mu^2/M^2 = 1.0$.

$\beta e^2 > 1$ [22], so we begin our analysis with the case of $\beta e^2 > 1$. We shall give comments for the possibility of finding the solution of $\beta e^2 < 1$ in the next subsection.

A. The solutions of the integrable sector

The analytic profiles (4.1) can be written in the coordinate y as

$$g(y) = \begin{cases} \frac{a^2 y}{a^2 y + 1 - y} & \text{for } n = 1 \\ \frac{a^4 y^2}{a^4 y^2 + (1-y)^2} & \text{for } n = 2, \end{cases} \tag{5.11}$$

where a is determined via (4.3). Apparently (5.1) are solutions of (5.1). Next, we will see whether the solutions appear or not when we numerically solve (5.1) without any constraint. Also, for the obtained solutions we will check the zero curvature condition (2.4).

Since (5.1) is an ordinary second order differential equation, of course there are several methods to investigate. However, it is easily noticed that Eq. (5.1) may exhibit singularlike behavior at the boundary because of the term $g(1-g)$ of the denominator. Once the computation contains a small numerical error, the equation quickly diverges. The numerical method which can safely solve such a difficulty is well known, the SOR method. Essentially, we have solved the following diffusion equation for a field $\tilde{g}(y, t)$:

$$\frac{\partial \tilde{g}}{\partial t} = \omega \mathcal{A}\left[\tilde{g}, \frac{\partial \tilde{g}}{\partial y}, \frac{\partial^2 \tilde{g}}{\partial y^2}\right], \tag{5.12}$$

in which we employ (5.1) as $\mathcal{A}$. Here ω is called a relaxation factor which is usually chosen as $\omega = 1.0$–2.0. After a huge number of iteration steps, the field is relaxed to the static one, i.e., $\tilde{g}(y, t) \to g(y)$, which we are finding.

The first case is $n = 1$. From (1.8), the explicit form of the potential is

$$V_{n=1} = \frac{\mu^2}{2}(1 - n_3)^4. \tag{5.13}$$

In Fig. 1 we present the numerical solution $g(y)$ and the corresponding Hamiltonian density $H(\rho)$ for $n = 1$. Figure 2 is the energy per unit length and its components for several values of βe^2 with fixed μ. The function $g(y)$ in Fig. 1 perfectly agrees with the analytical solution (5.11). We shall give a few comments for the components of the energy. For the integrable solution, the topological contribution of the energy, i.e., E_2, should be a constant. Also, $E_4^{(1)}$ is exactly zero for the integrable solution. The value of the component $E_4^{(1)}$ in the numerical solution is not exactly zero, but compatible with zero within the numerical precision. Note that the plot seems to blow up for the vicinity of $\beta e^2 = 1.0$, but the value is still up to order $\sim 10^{-8}$, so it is still negligible. This clearly means that our numerical solutions satisfy the zero curvature condition and thus belong to the integrable sector. These numerical errors probably originate in the finite number of the mesh points. In the usual case, we use the number $N_{\text{mesh}} = 1000$. When we employ a larger number, the value of E_2 should converge to the constant, i.e., 2π.

For $n = 2$, the form of the potential is

$$V_{n=2} = \frac{\mu^2}{2}(1 + n_3)(1 - n_3)^3; \tag{5.14}$$

thus, the potential is zero at both the origin and infinity. Figure 3 is the profile function and the Hamiltonian density for $n = 2$. Again, the numerical profile and the analytical one (5.11) coalesce. Contrary to the case of $n = 1$, the density has an annular shape. Figure 4 is the energy per unit length and its components for several values of βe^2 and fixed μ^2. Again, we confirmed that the value of the component $E_1^{(4)}$ is regarded as zero within the numerical uncertainty.

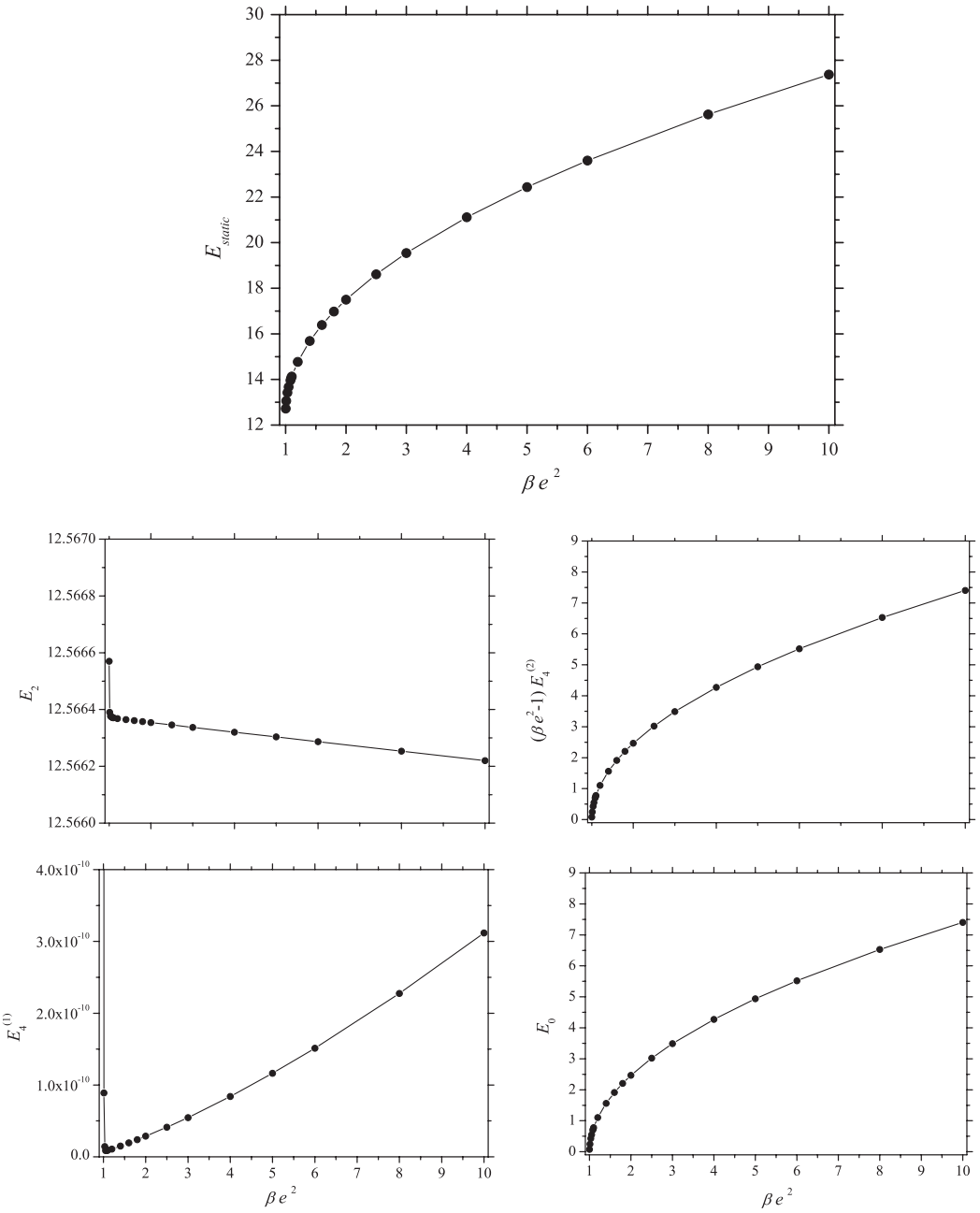

FIG. 4. The static energy and its components corresponding to the solutions of Fig. 3.

For $n = 3$, the form of the potential is

$$V_{n=3} = \frac{\mu^2}{2}(1 + n_3)^{4/3}(1 - n_3)^{8/3}; \tag{5.15}$$

thus, again, the potential is zero at both the origin and infinity. Figure 5 is the profile function and the Hamiltonian density for $n = 3$. As is easily seen, the radius of the annulus is larger than that of $n = 2$. Figure 6 is the energy per unit length and its components for several values of βe^2 and fixed μ^2. In this case, we face a numerical difficulty. During the computation by the SOR method, the solution g tends to oscillate around the true value, and sometimes it accidentally goes below zero at the vicinity of the origin, and then the computation fails because of the term $g^{1+2/n}$ in (5.1). In order to avoid it, we employ a finer mesh; i.e., the number is at least $N_{\text{mesh}} = 3000$.

Until now, we have examined the case of $\beta e^2 > 1$. The formalism leading to (4.3) suggests that the choice $\beta e^2 < 1$ and $\mu^2 < 0$ might also be possible, and the scale is now defined as

$$a = |n|\left[\frac{M^2(1 - \beta e^2)}{-r_0^2\mu^2}\right]^{1/4} \quad \text{for } \beta e^2 < 1, \qquad \mu^2 < 0. \tag{5.16}$$

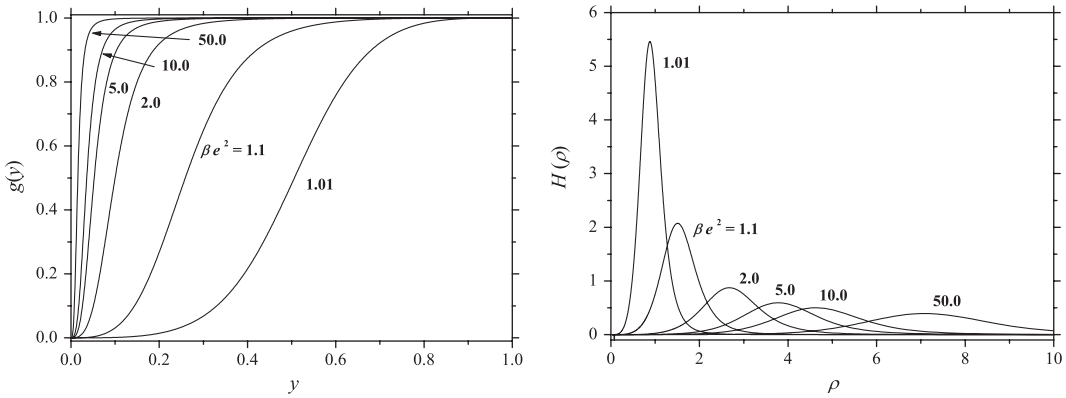

FIG. 5. The $n = 3$ profile $g(y)$ and the corresponding Hamiltonian density of the real space $H(\rho)$ of $k^2 = 0.0$ for the constant $r_0^2\mu^2/M^2 = 1.0$.

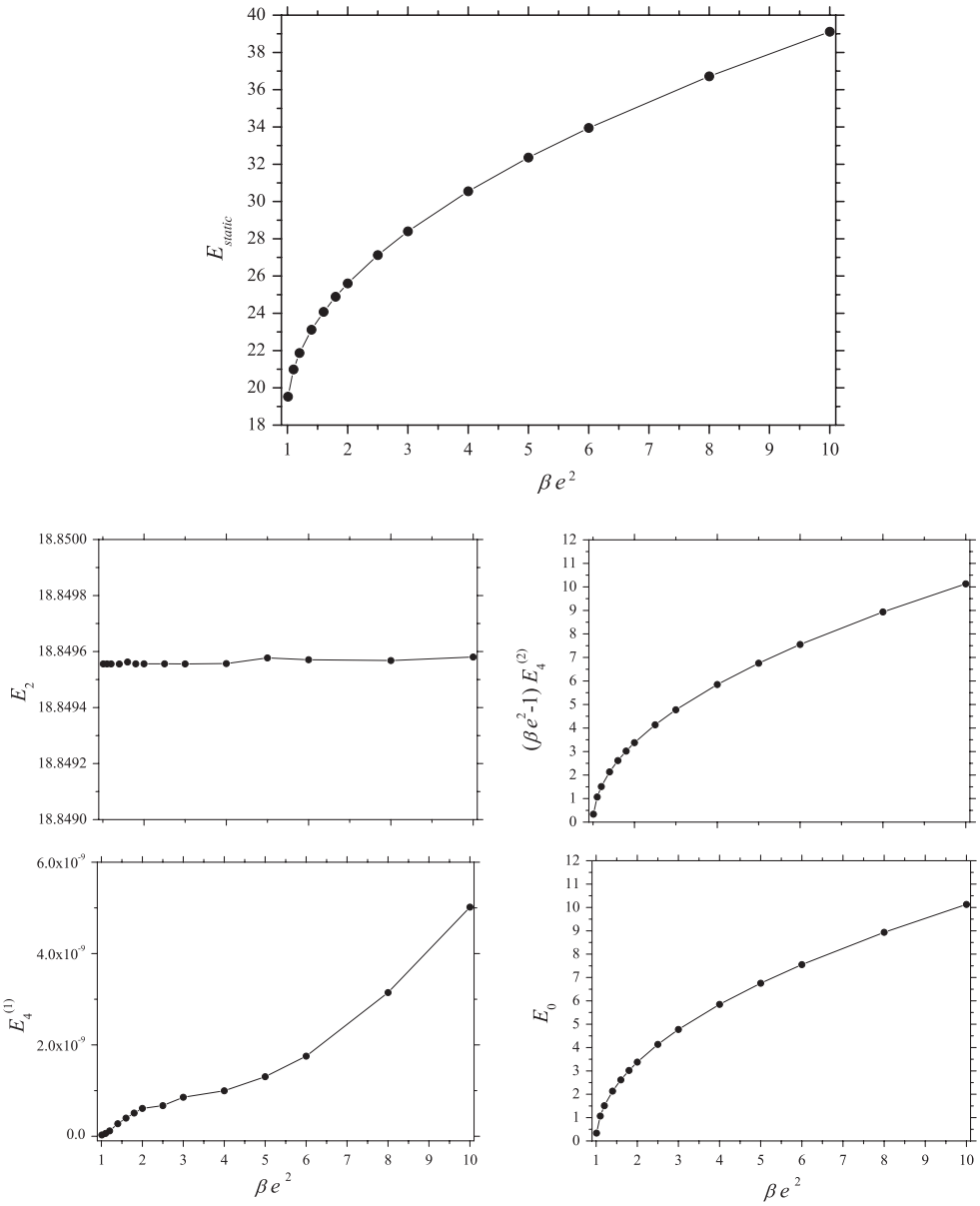

FIG. 6. The static energy and its components corresponding to the solutions of Fig. 5.

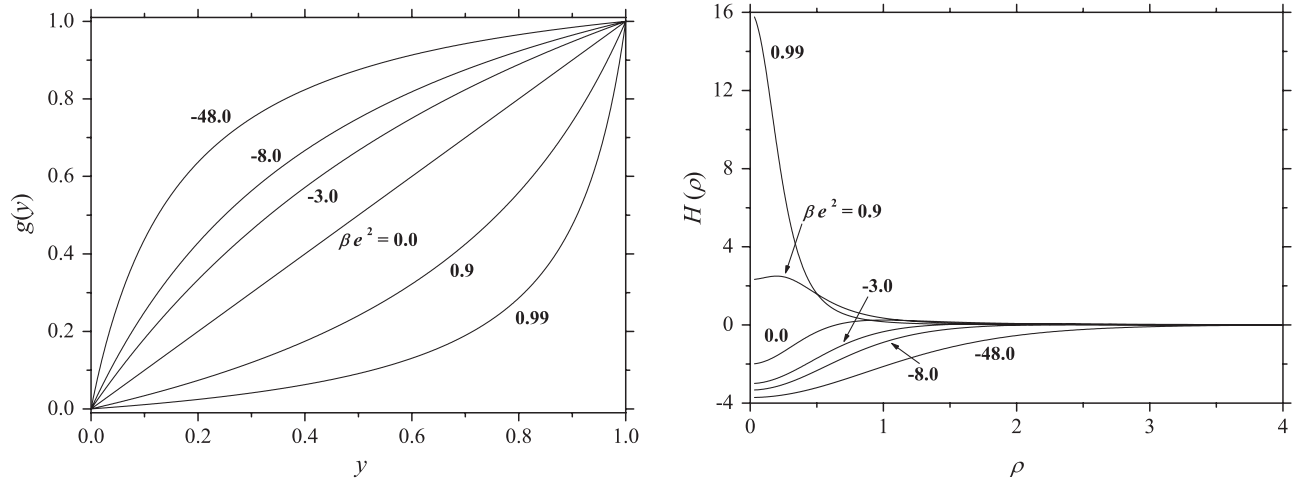

FIG. 7. The $n = 1$ profile functions and the energy density for the case of $\beta e^2 < 1$, for the constant $r_0^2\mu^2/M^2 = -1.0$.

The result is plotted in Fig. 7. However, the existence of such solutions seems dubious; the energy turns negative at a critical value of βe^2, and thus the solution has no lower energy bound. Also, numerically the change of sign of the potential in the equation of motion quickly breaks the computation.

B. The solutions outside of the integrable sector

Although we have obtained the analytical solutions for a special form of the potential (1.8), we have many options for the choice of the potential. The potentials which we employed in this paper essentially belong to a class of the generalized baby Skyrmion (BS) potentials formally written as

$$V_{\mathrm{BS}} = \frac{\mu^2}{2}\upsilon_\gamma^\alpha, \qquad \upsilon_\gamma^\alpha = (1+n_3)^\alpha(1-n_3)^\gamma. \tag{5.17}$$

For $\alpha = 0$, the potential is called (the class of) the *old*-BS potential which was introduced in [34], while $\alpha \neq 0$ is (the class of) the *new*-BS potential [35]. Our case (1.8) corresponds to $\alpha = 2 - 2/n$, $\gamma = 2 + 2/n$. Note that the possible choice of the potential is certainly restricted by the analysis of the limiting behavior (2.11) for several potentials. The results are summarized in Table I.

TABLE I. The analysis of the limiting behavior of the solutions at both $y = 0, 1$ for several choices of the potential, and ○ (×), which indicates that solutions exist (do not exist).

υ_γ^α	$n = 1$	$n = 2$	$n = 3$
Old-BS: $1 - n_3$	×	×	×
$(1 - n_3)^2$	×	○	○
$(1 - n_3)^3$	○	○	○
$(1 - n_3)^4$	○	○	○
New-BS: $(1 + n_3)(1 - n_3)$	×	×	×
$(1 + n_3)(1 - n_3)^3$	○	○	○
$(1 + n_3)^{4/3}(1 - n_3)^{3/8}$	○	○	○

We can obtain many numerical solutions for the several types of potentials. We show the result of $n = 2$ for the potentials υ_2^0, υ_4^0, $\upsilon_{8/3}^{4/3}$; of course, these are not of the form of the analytical solution. Figure 8 presents the energies and the component $E_4^{(1)}$ for these potentials. For $n = 2$, the *old*-BS potentials give higher total energy than the new one. This indicates that the same class of potentials gives similar energy, and then, for $n = 2$, the energy of the *new* type of potential $\upsilon_{8/3}^{4/3}$ is closest to the integrable sector, which is also plotted in Fig. 8 for reference.

VI. POTENTIAL PHYSICAL APPLICATIONS OF THE SOLUTIONS

Since the model (1.1) was proposed in the context of the Wilsonian renormalization group argument of the $SU(2)$ Yang-Mills theory, we expect that the vortex solutions constructed in this paper should describe some features of strong coupling regimes, such as the dual superconductor picture [36]. Apart from that, vortices appear in several areas of physics. The Nielsen-Olesen vortices in the Abelian Higgs model [37] were applied for type II superconductors (SC), and later they were extensively studied in the context of cosmology, i.e., the cosmic string [38] and the brane-world scenario [39]. The model has a close relationship with the standard electroweak theory, especially when one considers the case of a global $SU(2)$ and a local $U(1)$ breaking into a global $U(1)$, where the model reduces to an Abelian Higgs model with two charged scalar fields [40]. It is interesting to note that the vortices of such a model carry the so-called longitudinal electromagnetic currents [41,42].

In (4.4) we give the Noether current associated with a global $U(1)$, i.e., $u \to e^{i\alpha}u$, and so one can

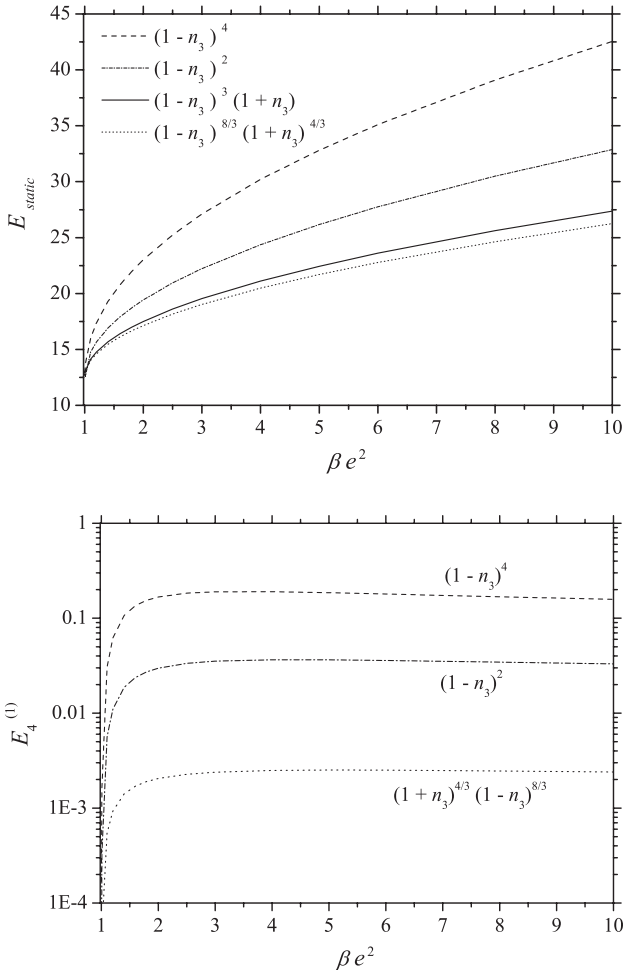

FIG. 8. The $n = 2$ static energy and the component $E_4^{(1)}$ for several types of potentials, v_j^i. $k^2 = 0$ and $r_0^2\mu^2/M^2 = 1.0$.

straightforwardly compute the longitudinal current in the integrable/nonintegrable sector. In Fig. 9, we plot the typical results of the transverse spatial structure of the polar component of the current in the case of the integrable sector. [Using (4.1) and (4.4), one can easily see that the radial component of the current is always zero.] Note that for higher winding numbers as well for unit winding numbers, the solutions exhibit a pipelike structure, which was observed in the analysis of [43].

Our model enjoys a symmetry breaking of the type $O(3)_{\text{global}} \to O(2)_{\text{global}}$, which is similar to $SU(2)_{\text{global}} \otimes U(1)_{\text{local}} \to U(1)_{\text{global}}$. A notable difference between the Nielsen-Olesen vortices and ours is that the gauge degrees of freedom are absent in our model. If one wishes to discuss the existence of the gauge field in type II SC, however, the gauging of the model according to [44] should work. Confinement or squeezing of the magnetic field into type II SC should be realized in terms of the localization of the gauge field into our vortices.

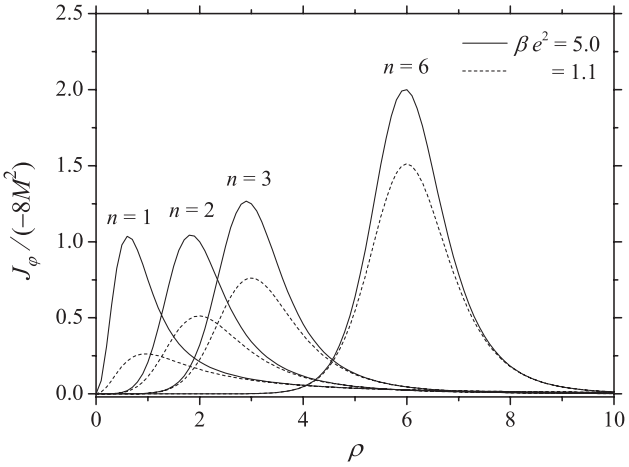

FIG. 9. The transverse spatial structure of the polar component of the currents (in units of $-1/8M^2$) for the topological charge $n = 1$, 2, 3, and 6, with the parameters $\beta e^2 = 1.1$, 5.0. We set $r_0^2\mu^2/M^2 = 1.0$. All solutions have a pipelike structure.

VII. SUMMARY

We have studied vortex solutions of the extended Skyrme-Faddeev model, especially for the outside of the integrable constraint $\beta e^2 = 1$. In order to find the solutions, we introduced potentials of the extension of the baby Skyrmion type. We found several analytical solutions of the model. We also confirmed the existence of the solutions in terms of the numerical analysis. By using the standard SOR method, we obtained the axially symmetric solutions for charge up to $n = 3$ with several forms of the potential for various values of the model parameters.

In this work, we imposed the axial symmetry to the solution ansatz. However, solutions with lower symmetry, such as $\mathbb{Z}_2$ symmetry, were found by a numerical simulation for the baby Skyrme model [45]. It would be interesting to investigate whether such deformed solutions appear in the extended Skyrme-Faddeev model. Furthermore, full 3D simulations of the model will certainly clarify the detailed structure of the vortices. The analysis implementing these issues will be discussed in a forthcoming paper.

ACKNOWLEDGMENTS

We are grateful to the anonymous referee for a careful reading of the manuscript and for valuable remarks on the physical applications. We would like to thank Wojtek Zakrzewski and Paweł Klimas for many useful discussions. N. S. would like to thank the kind hospitality at Instituto de Física de São Carlos, Universidade de São Paulo. He also acknowledges the financial support of FAPESP (Brazil). J. J. would also like to thank the UK Engineering and Physical Sciences Research Council for support. L. A. F. is partially supported by CNPq-Brazil.

[1] L. D. Faddeev, in *40 Years in Mathematical Physics* (World Scientific, Singapore, 1995).

[2] A. M. Polyakov and A. A. Belavin, JETP Lett. **22**, 245 (1975).

[3] J. Gladikowski and M. Hellmund, Phys. Rev. D **56**, 5194 (1997).

[4] L. D. Faddeev and A. J. Niemi, Nature (London) **387**, 58 (1997); arXiv:hep-th/9705176.

[5] R. A. Battye and P. M. Sutcliffe, Phys. Rev. Lett. **81**, 4798 (1998); Proc. R. Soc. A **455**, 4305 (1999).

[6] J. Hietarinta and P. Salo, Phys. Lett. B **451**, 60 (1999); Phys. Rev. D **62**, 081701(R) (2000).

[7] E. Babaev, L. D. Faddeev, and A. J. Niemi, Phys. Rev. B **65**, 100512(R) (2002); E. Babaev, Phys. Rev. Lett. **88**, 177002 (2002).

[8] P. Sutcliffe, Proc. R. Soc. A **463**, 3001 (2007); J. Hietarinta, J. Jäykkä, and P. Salo, Phys. Lett. A **321**, 324 (2004); J. Jäykkä and J. Hietarinta, Phys. Rev. D **79**, 125027 (2009).

[9] J. Hietarinta, J. Palmu, J. Jäykkä, and P. Pakkanen, New J. Phys. **14**, 013013 (2012).

[10] L. D. Faddeev and A. J. Niemi, Phys. Rev. Lett. **82**, 1624 (1999).

[11] Y. M. Cho, Phys. Rev. D **21**, 1080 (1980); **23**, 2415 (1981).

[12] L. Dittmann, T. Heinzl, and A. Wipf, Nucl. Phys. B, Proc. Suppl. **106-107**, 649 (2002); **108**, 63 (2002).

[13] L. D. Faddeev, arXiv:0805.1624; L. D. Faddeev and A. J. Niemi, Nucl. Phys. **B776**, 38 (2007).

[14] H. Gies, Phys. Rev. D **63**, 125023 (2001).

[15] L. A. Ferreira, J. High Energy Phys. 05 (2009) 001.

[16] L. A. Ferreira, P. Klimas, and W. J. Zakrzewski, J. High Energy Phys. 12 (2011) 098.

[17] L. A. Ferreira and P. Klimas, J. High Energy Phys. 10 (2010) 008.

[18] L. A. Ferreira, P. Klimas, and W. J. Zakrzewski, Phys. Rev. D **83**, 105018 (2011).

[19] L. A. Ferreira, P. Klimas, and W. J. Zakrzewski, Phys. Rev. D **84**, 085022 (2011).

[20] A. Kundu and Y. P. Rybakov, J. Phys. A **15**, 269 (1982); C.-G. Shi and M. Hirayama, Int. J. Mod. Phys. A **23**, 1361 (2008).

[21] N. Sawado, N. Shiiki, and S. Tanaka, Mod. Phys. Lett. A **21**, 1189 (2006).

[22] L. A. Ferreira, N. Sawado, and K. Toda, J. High Energy Phys. 11 (2009) 124.

[23] L. A. Ferreira, N. Sawado, and K. Toda, J. Phys. A **43**, 434014 (2010).

[24] L. A. Ferreira, S. Kato, N. Sawado, and K. Toda, Acta polytechnica Scandinavica Physics including nucleonics series **51**, 47 (2011).

[25] O. Babelon and L. A. Ferreira, J. High Energy Phys. 11 (2002) 020.

[26] P. Eslami, W. J. Zakrzewski, and M. Sarbishaei, Nonlinearity **13**, 1867 (2000).

[27] C. Adam, T. Romanczukiewicz, J. Sanchez-Guillen, and A. Wereszczynski, Phys. Rev. D **81**, 085007 (2010).

[28] O. Alvarez, L. A. Ferreira, and J. Sanchez Guillen, Nucl. Phys. **B529**, 689 (1998).

[29] O. Alvarez, L. A. Ferreira, and J. Sanchez-Guillen, Int. J. Mod. Phys. A **24**, 1825 (2009).

[30] L. A. Ferreira and A. V. Razumov, Lett. Math. Phys. **55**, 143 (2001).

[31] C. Adam, J. Sanchez-Guillen, and A. Wereszczynski, J. Math. Phys. (N.Y.) **47**, 022303 (2006).

[32] L. A. Ferreira and A. C. Risério do Bonfim, J. High Energy Phys. 10 (2010) 119.

[33] See, e.g., I. S. Gradshteyn and I. M. Ryzhik, *Tables of Integrals, Series, and Products* (Academic Press, London, 2007), 7th ed.

[34] R. A. Leese, M. Peyrard, and W. J. Zakrzewski, Nonlinearity **3**, 773 (1990).

[35] A. E. Kudryavtsev, B. M. A. Piette, and W. J. Zakrzewski, Nonlinearity **11**, 783 (1998).

[36] Y. Nambu, Phys. Rev. D **10**, 4262 (1974); S. Mandelstam, Phys. Rep. **23**, 245 (1976); G. 't Hooft, Nucl. Phys. **B190**, 455 (1981).

[37] H. B. Nielsen and P. Olesen, Nucl. Phys. **B61**, 45 (1973).

[38] M. B. Hindmarsh and T. W. B. Kibble, Rep. Prog. Phys. **58**, 477 (1995).

[39] M. Giovannini, H. Meyer, and M. E. Shaposhnikov, Nucl. Phys. **B619**, 615 (2001).

[40] A. Achucarro and T. Vachaspati, Phys. Rep. **327**, 347 (2000).

[41] P. Forgacs, S. Reuillon, and M. S. Volkov, Nucl. Phys. **B751**, 390 (2006).

[42] M. S. Volkov, Phys. Lett. B **644**, 203 (2007).

[43] M. N. Chernodub and A. S. Nedelin, Phys. Rev. D **81**, 125022 (2010).

[44] J. Gladikowski, B. M. A. Piette, and B. J. Schroers, Phys. Rev. D **53**, 844 (1996).

[45] I. Hen and M. Karliner, Nonlinearity **21**, 399 (2008).